**Fei-Yue Wang**
Robotics and Automation Laboratory
Department of Systems and Industrial Engineering
The University of Arizona, Tucson, Arizona 85721
E-mail: feiyue@apache.sie.arizona.edu

# On the Extremal Fundamental Frequencies of One-Link Flexible Manipulators

## Abstract

*The problem of maximizing the fundamental vibration frequency of a flexible manipulator through the optimum design of its link is addressed. A larger fundamental vibration frequency is desired because it will enable the manipulator to move faster without causing serious oscillation of its end point. Using the variational method, we show that this design problem can be formulated as a nonlinear eigenvalue problem and thus solved by a set of successive iteration schemes. Sensitivity analysis for the optimum design is also performed to obtain useful information for machining allowance specifications. The results of this investigation should be very useful in the design of lightweight and high-performance robotic arms. For example, numeric calculations indicated that an increase ranging from 194.92% to 600.25% in the fundamental vibration frequency can be achieved by the optimum tapering of a flexible manipulator with a link of geometrically similar cross sections. This may lead to a significant improvement in productivity, as the manipulator can rotate three to seven times faster.*

## 1. Introduction

One of the major objectives for developing flexible or lightweight manipulators is to achieve high speed and high precision performance. When the joint velocity of a flexible manipulator approaches its fundamental vibration frequency, however, the intensity of oscillations of its end point will increase dramatically as a result of resonance. This will cause a serious problem in controlling the end-point position or even damage to the manipulator system. Thus, a larger fundamental vibration frequency is desired for flexible manipulators.

Asada et al. (1991) have investigated the problem of integrated structure/control design of flexible manipulators. They found that for a flexible manipulator with a beam (or link) of varying rectangular cross sections, a 43% increase in the fundamental vibration frequency can be achieved by tapering the beam appropriately. Their result may have a significant impact on the design of flexible manipulators, since to date most of them have been constructed with uniform beams of regular and conventional cross sections (e.g., uniform rectangular cross sections).

The problem of optimum shape design of flexible manipulators is clearly related to the optimum design of vibrating elastic structures, especially vibrating rods and beams (Schwarz 1962; Niordson 1965). For example, as we can see later in Section 4, when the hub inertia of a flexible manipulator approaches infinity, the problem of finding the extremal fundamental frequency of the manipulator will be reduced to the classic problem of optimum design of a vibrating cantilever, which was first formulated and solved by Karihaloo and Niordson (1973) and has been reexamined by Wang (1991) with a new and simplified solution procedure. It was found that for a cantilever of geometrically similar cross sections, a 578% increase in the fundamental frequency can be obtained through optimum shape design.

The goal of this article is to generalize the solution method developed for vibrating cantilevers to solve the optimum design problem of flexible manipulators. We start with the basic equations of one-link flexible manipulators in Section 2 and present the variational formulation of the shape design problem in Section 3. The optimal solutions in the two limiting situations and their behaviors near the singular points are analyzed in Section 4. Section 5 describes a set of successive iteration schemes for solving the nonlinear eigenvalue problem of the optimum design for various conditions, followed by a number of numeric examples and discussion in Section 6. Changes

The International Journal of Robotics Research,
Vol. 13, No. 2, April 1994, pp. 162-170,

in the optimal fundamental frequency caused by small variations of the hub inertia are investigated in Section 7 by introducing a sensitivity index. Section 8 concludes the article.

## 2. Basic Vibration Equations of One-Link Flexible Manipulators

The Euler-Bernoulli equations have been widely used in the literature to describe the dynamics of flexible manipulators (Bellezze et al. 1990; Wang and Kwan 1993). In this model, a one-link flexible manipulator is made of a simple beam and an actuator fixed on a hub with rotational inertia $I_H$. The governing equation of harmonic vibration and boundary conditions can be easily derived as,

$$(EIv'')'' - \rho A\omega^2 v = 0, \tag{1}$$

$$v(0) = 0, \qquad I_H\omega^2 v'(0) + EIv''(0) = 0, \tag{2}$$
$$EIv''(L) = 0, \quad (EIv'')'(L) = 0$$

where $v$ is the total beam displacement; $EI$, the bending rigidity; $A$, the cross-sectional area; $\rho$, the mass density per unit volume; $L$, the length; and $\omega$, the natural vibration frequency. Primes indicate derivatives with respect to the coordinate $x$ of the beam's longitudinal axis.

For a manipulator with beams of uniform cross sections, its fundamental vibration frequency is determined as the minimum root of the following characteristic equation,

$$\sin\theta\cosh\theta - \cos\theta\sinh\theta + \eta\theta^3(1 + \cosh\theta\cos\theta) = 0, \tag{3}$$

$$\omega = \sqrt{\frac{EI}{\rho A}}\left(\frac{\theta}{L}\right)^2, \quad \eta = \frac{I_H}{\rho AL^3},$$

and the corresponding vibration mode is,

$$v(x) = \sinh\theta\sin\frac{\theta x}{L} + \sin\theta\sinh\frac{\theta x}{L} + \frac{\eta\theta^3}{2}\left[\sin\theta(1 - \frac{x}{L}) - \sinh\theta(1 - \frac{x}{L}) + \sinh\theta\cos\frac{\theta x}{L} - \cosh\theta\sin\frac{\theta x}{L} + \cos\theta\sinh\frac{\theta x}{L} - \sin\theta\cosh\frac{\theta x}{L}\right] \tag{4}$$

It is easy to show that $\theta$ increases monotonically as $\eta$ decreases and $1.8751 \le \theta \le 3.9266$. The lower and upper bounds of $\theta$ are achieved at $\eta = \infty$ and $\eta = 0$, respectively. Note that when $\eta = \infty$, eq. (3) reduces to the characteristic equation of a clamped cantilever, whereas when $\eta = 0$, it becomes that of a hinged cantilever.

For manipulators with a beam of varying cross sections, however, the simple equations like eqs. (3)–(4) for the fundamental frequency are no longer possible. In this case, the fundamental frequency is a nonlinear functional of the shape function. Our objective here is to find the best possible tapering of the beam such that a manipulator will obtain its highest possible fundamental vibration frequency.

Throughout this article we will assume the following relationship between the moment $I$ and the area $A$ of beam cross sections:

$$I(x) = \gamma A^p(x), \qquad p \ge 1 \tag{5}$$

where $\gamma$ is a constant. Three cases are of special interest—namely, $p$=1, 2, and 3—since they correspond to beams with rectangular cross sections of given uniform height, geometrically similar cross sections, and rectangular cross sections of given uniform width, respectively.

## 3. Variational Formulation for Optimum Shape Design

To establish the basic equations for solving the optimum shape design problem, we reformulate eqs. (1)–(2) into the following variational form,

$$\omega^2 = \min_v \frac{\int_0^L EIv''^2 dx}{\int_0^L \rho Av^2 dx + I_H v'(0)^2}, \tag{6}$$

where $v$ only needs to satisfy the *geometric* boundary condition $v(0) = 0$. The equivalence of eq. (6) and eqs. (1)–(2) can be easily proved.

Based on eq. (5), the problem of optimum shape design now can be stated as a variational problem in the following dimensionless form,

$$\lambda = \max_\alpha \min_v \frac{\int_0^1 \alpha^p v''^2 d\xi}{\int_0^1 \alpha v^2 d\xi + \eta v'(0)^2}, \tag{7}$$

where the dimensionless coordinate $\xi$, eigenvalue $\lambda$, shape function $\alpha$, and hub inertia parameter $\eta$ are defined, respectively, by,

$$\xi = \frac{x}{L}, \quad \lambda = \frac{\rho^p L^{3+p}}{\gamma E W^{p-1}}\omega^2, \quad \alpha = \frac{\rho LA}{W}, \quad \eta = \frac{I_H}{WL^2}; \tag{8}$$

in which $W$ is the given total weight of the beam. From the definition, $\alpha$ must be non-negative and satisfy the following constraint:

$$\int_0^1 \alpha d\xi = 1. \tag{9}$$

To incorporate this constraint into eq. (7), we introduce a generalized variational equation through a Lagrange multiplier as follows,

$$\lambda^* = \max_\alpha \min_v \frac{\int_0^1 \alpha^p v''^2 d\xi}{\int_0^1 \alpha v^2 d\xi + \eta v'(0)^2 + \sigma^2(\int_0^1 \alpha d\xi - 1)}, \tag{10}$$

where $\sigma^2$ is the Lagrange multiplier and must be positive.

After some long and tedious calculus, one can show that the generalized variational equation leads to the following Euler equations,

$$(\alpha^p v'')'' - \lambda\alpha v = 0, \tag{11}$$

$$p\alpha^{p-1}(v'')^2 - \lambda v^2 = \lambda\sigma^2, \tag{12}$$

and boundary conditions,

$$v(0) = 0, \quad \alpha^p v''(0) + \lambda\eta v'(0) = 0; \tag{13}$$
$$\alpha^p v''(1) = 0, \quad (\alpha^p v'')'(1) = 0.$$

These equations, together with constraint (9), form the complete set of basic equations of the optimum shape design for a one-link flexible manipulator.

Clearly, the solution of eqs. (11)–(13) is not unique, because if $(v, \sigma^2, \alpha, \lambda)$ is a solution, then $(cv, c^2\sigma^2, \alpha, \lambda)$ will be another solution for any nonzero constant $c$. This provides a way to completely eliminate the multiplier from (12) by choosing $c = 1/\sigma$. In other words, for solving the optimization problem, we only need to find the unknown function $u = v/\sigma$ instead of $v$ and $\sigma^2$ individually. In terms of this new function $u$, eqs. (11)–(13) can be rewritten as,

$$(\alpha^p u'')'' - \lambda\alpha u = 0, \tag{14}$$

$$p\alpha^{p-1}(u'')^2 - \lambda u^2 = \lambda, \tag{15}$$

$$u(0) = 0, \quad \alpha^p u''(0) + \lambda\eta u'(0) = 0; \tag{16}$$
$$\alpha^p u''(1) = 0, \quad (\alpha^p u'')'(1) = 0.$$

These equations constitute a nonlinear eigenvalue problem for finding the frequency $\lambda$. Obtaining the optimum shape for a flexible manipulator is equivalent to finding an $\alpha$ that maximizes the smallest eigenvalue of eqs. (14)–(16), subject to constraint (9).

Comparing eqs. (14)–(16) with the corresponding ones for the optimum design of vibrating cantilevers (Karihaloo and Niordson 1973), one finds that the only difference between them is in the second equation of boundary conditions (16). For vibrating cantilevers, this equation becomes $u'(0) = 0$ and leads to a substantial simplification of the solution procedure. The reason is in this case both $u(0)$ and $u'(0)$ are known, and hence $u(\xi)$ can be found uniquely from $u''(\xi)$ by integration. For flexible manipulators, however, $u'(0)$ cannot be known from the boundary conditions. Thus $u(\xi)$ cannot be determined directly from $u''(\xi)$ by integration, and successive iterations must be used. As one can see from the next two sections, this complicates the solution procedure and slows down the speed of convergences significantly.

From eq. (15), for $p > 1$, one finds,

$$\alpha(\xi) = \frac{\phi_u(\xi)}{\beta}, \tag{17}$$

where

$$\phi_u(\xi) = \left[\frac{u^2(\xi) + 1}{u''^2(\xi)}\right]^{\frac{1}{p-1}}, \quad \beta = \left(\frac{p}{\lambda}\right)^{\frac{1}{p-1}}, \quad \lambda = \frac{p}{\beta^{p-1}}. \tag{18}$$

Another important identity can be obtained by multiplying both sides of eq. (14) by $u$ and then integrating over $0 \le \xi \le 1$. Taking boundary conditions (16) into account and after applying eq. (15), we have,

$$\int_0^1 \alpha(\xi)d\xi = (p-1)\int_0^1 \alpha(\xi)u(\xi)^2 d\xi + p\eta u'(0)^2 \tag{19}$$

Note that the validity of this identity does not require constraint (9) to hold.

## 4. Limiting Cases and Singularity Analysis

Before we attempt to solve the nonlinear eigenvalue problem (14)–(16), it is expedient to investigate the solutions in the limiting cases with respect to $\eta$. For the purpose of numeric computation, it is also imperative to analyze the singularity of solutions at the free end ($\xi = 1$) or the clamped end ($\xi = 0$). We will show that for $p = 1$ and $\eta = 0$ or $\infty$, no optimal solution exists; for $p > 1$ and $\eta \neq 0$, the optimal solution is singular at the free end; and for $p > 1$ and $\eta = 0$, the solution is singular at both the free and clamped ends. Furthermore, as expected, for very large $\eta$, the optimum design problem reduces to the corresponding one for vibrating cantilevers.

### *4.1. Two Limiting Cases*

Let us consider two limiting cases in which $\eta = 0$ and $\eta = \infty$, respectively. For $\eta = 0$, the second equation of boundary conditions (16) becomes,

$$\alpha^p u''(0) = 0, \tag{20}$$

and identity (19) now reads,

$$\int_0^1 \alpha(\xi)\, d\xi = (p-1)\int_0^1 \alpha(\xi)u(\xi)^2\, d\xi. \tag{21}$$

Therefore, no optimal solution is possible for $p = 1$, since constraint (9) cannot be satisfied by any solution. For $p > 1$, as it can be shown shortly, eq. (20) leads to the singularity of the optimal solution at the clamped end $\xi = 0$.

For $\eta = \infty$, the second equation of (16) has to be replaced by,

$$u'(0) = 0,$$

and all the other equations in (14)–(16) remain unchanged. Clearly, both the governing equations and

boundary conditions now become exactly the same as those for the optimum design of vibrating cantilevers (Karihaloo and Niordson 1973). Thus the optimization problem in this case reduces to that of cantilevers. It is easy to show that in this case, identity (19) also reduces to (21). Hence, for the same reason, no optimal solution exists when $p = 1$.

### 4.2. *Singularity Analysis*

When $p \neq 1$, the solution of eqs. (14)–(16) is singular at the free end for $\eta \neq 0$ and at both the free and clamped ends for $\eta = 0$. In this case the numeric method cannot be applied to find the solution directly. To make the numeric solution feasible, we must first determine the behavior of the solution near these singular points. This can be achieved by assuming that the solution can be expanded in a power series of $\xi$ or $1 - \xi$ with a characteristic term $\xi^k$ or $(1 - \xi)^k$ near the singular points.

To analyze the singularity at the free end, let us expand both $u$ and $\alpha$ in a power series of $1 - \xi$ at $\xi = 1$,

$$u(\xi) = u_0(1 - \xi)^k + \cdots, \quad \alpha(\xi) = a_0(1 - \xi)^m + \cdots. \tag{22}$$

Substituting these expressions into (15), we get,

$$2k = m(p - 1) + 2(k - 2), \qquad \lambda = pa_0^{p-1}k^2(k - 1)^2.$$

Similarly, we have from (14),

$$\lambda a_0 = a_0^p k(k - 1)(m + k + 2)(m + k + 1).$$

Eliminating $\lambda$ and $a_0$ from those equations, we find,

$$m = \frac{4}{p - 1}, \tag{23}$$

$$[k(p - 1) + 2(p + 1)][k(p - 1) + p + 3] \tag{24}$$
$$-p(p - 1)^2k(k - 1) = 0.$$

For $p = 2$, we get $k = -2$, and for $p = 3$, $k = -1$.

For $\eta = 0$, the solution of (14)–(16) is also singular at $\xi = 0$. To determine the singularity at this point, we notice the following facts when $\eta = 0$,

$$\alpha^p u''(0) = 0, \qquad \alpha^{p-1}u''^2(0) = \text{ finite.}$$

Therefore, the series expansions for those two functions near $\xi = 0$ can be written as,

$$\alpha^p u'' = a_1\xi + a_2\xi^2 + \cdots, \quad \alpha^{p-1}u''^2 = b_1 + \cdots,$$

where $a_1, a_2$, and $b_1$ are constants. Solving the above equations for $\alpha$ and $u''$ we get,

$$\alpha(\xi) = c_1\xi^{\frac{2}{p+1}} + \cdots, \tag{25}$$
$$u''(\xi) = d_1\xi^{-\frac{p-1}{p+1}} + \cdots, \tag{26}$$

where $c_1$ and $d_1$ are two new constants. The behavior of $u$ near the clamped end thus can be found as

$$u(\xi) = d_1\xi^{\frac{p+3}{p+1}} + \cdots. \tag{27}$$

Therefore, the singularity of $u$ at $\xi = 0$ is $k = p + 3/p + 1$.

The results of singularity analysis will be used to normalize the functions employed in the iteration schemes developed in the next section.

## 5. Solution by Successive Iterations

Since in general the solution of the nonlinear eigenvalue problem (14)–(16) cannot be obtained in a closed form, a set of successive iteration schemes is developed to find it numerically. The iteration schemes are based on formal integration, with the introduction of one of the boundary conditions at each integration. Care is taken to remove the singularity of the solution at the singular points and to separate the differential operator of the highest order on the left-hand side at each step. This has been found necessary to make the numeric computation feasible and to achieve the convergence by successive iteration.

The following integral formulae are useful in the formulation of iteration schemes,

$$\int_0^\xi \int_0^x G(s)dsdx = \xi^2 \int_0^1 (1 - x)G(x\xi)\,dx, \tag{28}$$

$$\int_\xi^1 \int_x^1 G(s)dsdx = (1 - \xi)^2 \int_0^1 xG[\xi + x(1 - \xi)]\,dx. \tag{29}$$

Note that the single integrations save computation time and hence are preferred numerically over the double integrations.

For $p > 1$, by formal integration of (14) we find, after satisfying the boundary conditions at $\xi$=1, substituting $\alpha$ from (17) into (14), and using (29), that

$$u''(\xi) = \tag{30}$$
$$\frac{s\left[u^2(\xi) + 1\right]^{p/(p+1)}}{\left\{\begin{array}{c} p(1 - \xi)^2 \int_0^1 x\phi_u[\xi + x(1 - \xi)] \\ \times u[\xi + x(1 - \xi)]\,dx \end{array}\right\}^{(p-1)/(p+1)}}$$

where $s$ is a sign indicator defined as,

$$s = \text{sign}\left[\int_0^1 x\phi_u[\xi + x(1 - \xi)]u[\xi + x(1 - \xi)]\,dx\right]$$

Eq. (30) is used as the basic formula for constructing the iteration schemes for $p > 1$.

### 5.1. *Case* $p = 1$

For $p = 1$, function $\alpha$ drops out of eq. (15) and we have a degenerate case. Eqs. (14)–(16) now have the form,

$$(\alpha u'')'' - \lambda \alpha u = 0, \tag{31}$$

$$(u'')^2 = \lambda(u^2 + 1), \tag{32}$$

$$u(0) = 0, \quad \alpha u''(0) + \lambda \eta u'(0) = 0; \tag{33}$$

$$\alpha u''(1) = 0, \quad (\alpha u'')'(1) = 0.$$

And identity (19) becomes,

$$\eta u'(0)^2 = \int_0^1 \alpha(\xi)\, d\xi.$$

Since no solution exists for $\eta = 0$ or $\infty$, we consider only $0 < \eta < \infty$. In this case if we choose

$$\eta = \frac{1}{u'(0)^2}, \tag{34}$$

then $\alpha$ obtained by solving eq. (31) with boundary conditions in (33) must satisfy constraint (9) automatically. This observation leads to an *inverse* approach to solve the problem for $p = 1$. In other words, for a given $\lambda$ we determine $u$ and $\alpha$ by solving (31)–(33) with $\eta$ calculated from (34). This will establish a relationship between $\eta$ and the optimum eigenvalue $\lambda$, which in turn will enable us to find $\lambda$ for a given $\eta$ and hence solve the real optimization problem inversely.

To develop a successive iteration scheme, we formally integrate (31) and (32) with boundary conditions (33). Application of formulas (28) and (29) leads to,

$$u(\xi) = \xi u'(0) + \sqrt{\lambda}\xi^2 \int_0^1 (1 - x)\sqrt{u^2(x\xi) + 1}\, dx, \tag{35}$$

$$\alpha(\xi) = \sqrt{\lambda}\frac{(1 - \xi)^2}{\sqrt{u^2(\xi) + 1}} \int_0^1 x\alpha u[\xi + x(1 - \xi)]\, dx. \tag{36}$$

After application of (34), the second equation of (33) can be replaced by,

$$u'(0) = -\frac{1}{\int_0^1 x\alpha(x)u(x)\, dx}. \tag{37}$$

Based on eqs. (35)–(37), the iteration scheme can be outlined as follows,

1. For a given $\lambda$, select initial $u_0'(0)$, $u_0(\xi)$, and $\alpha_0(\xi)$.
2. Update $u_i$ according to:

$$u_{i+1}(\xi) = \xi u_i'(0) + \sqrt{\lambda}\xi^2 \int_0^1 (1 - x)\sqrt{u_i^2(x\xi) + 1}\, dx.$$

3. Update $\alpha_i$ according to:

$$\alpha_{i+1}(\xi) = \sqrt{\lambda}\frac{(1 - \xi)^2}{\sqrt{u_{i+1}^2(\xi) + 1}} \int_0^1 x\alpha_i u_{i+1}[\xi + x(1 - \xi)]\, dx.$$

4. Update $u_i'(0)$ according to:

$$u_{i+1}'(0) = -\frac{1}{\int_0^1 x\alpha_{i+1}(x)u_{i+1}(x)\, dx}.$$

5. If a given accuracy is not satisfied, go back to Step 2.

### 5.2. *Case* $p > 1$ *and* $\eta = 0$

Since the singularity cannot be dealt with directly in numeric computations, we introduce the following two new functions for $u$ and $u''$, respectively:

$$f(\xi) = (1 - \xi)^k u(\xi), \tag{38}$$

$$z(\xi) = \xi^{(p-1)/(p+1)}(1 - \xi)^{k+2}u''(\xi),$$

where $k$ is the singularity of $u$ at $\xi = 1$ determined from (24). Both $f$ and $z$ are regular over the entire interval $0 \le \xi \le 1$. It is easy to show that

$$f(0) = 0, \quad f'(0) = u'(0), \quad f(1) = \frac{z(1)}{k(k + 1)}. \tag{39}$$

In terms of $f$ and $z$, function $\phi_u$ can be rewritten as,

$$\phi_u(\xi) = \xi^{\frac{2}{p+1}}(1 - \xi)^{\frac{4}{p-1}}\phi(\xi), \tag{40}$$

$$\phi(\xi) = \left[\frac{f^2(\xi) + (1 - \xi)^{2k}}{z^2(\xi)}\right]^{1/(p-1)},$$

and hence according to constraint (9) parameter $\beta$ becomes,

$$\beta = \int_0^1 \xi^{\frac{2}{p+1}}(1 - \xi)^{\frac{4}{p-1}}\phi(\xi)d\xi. \tag{41}$$

By formal integration of (38) and after application of (28), we get,

$$f(\xi) = \xi(1 - \xi)^k \left[f'(0) + \xi^{2/(p+1)} \times \int_0^1 \frac{(1 - x)z(x\xi)}{x^{(p-1)/(p+1)}(1 - x\xi)^{k+2}}\, dx\right] \tag{42}$$

$$= \xi(1 - \xi)^k \left[f'(0) + (p + 1)/2\xi^{2/(p+1)} \times \int_0^1 \frac{(1 - x^{(p+1)/2})z(\xi x^{(p+1)/2})}{(1 - \xi x^{(p+1)/2})^{k+2}}\, dx\right],$$

$$0 \le \xi < 1$$

Note that the second expression of $f(\xi)$ removes the pseudosingularity of the integrand at $\xi = 0$. Substitution of (38) into (30) gives the following equation for $z$:

$$z(\xi) = \frac{s\xi^{(p-1)/(p+1)}\left[f^2(\xi) + (1-\xi)^{2k}\right]^{p/(p+1)}}{\left|\begin{array}{l} p\int_0^1 x(1-x)^{4/(p-1)-k} \\ \quad \times [\xi + x(1-\xi)]^{(p-1)/(p+1)} \\ \quad \times \phi[\xi + x(1-\xi)] f[\xi + x(1-\xi)]\, dx \end{array}\right|^{(p-1)/(p+1)}} \tag{43}$$

where $s$ is the sign of the denominator. The expression for $u'(0)$ can be found from boundary condition $\alpha^p u''(0) = 0$ as,

$$f'(0) = \frac{\int_0^1 x^{(p+3)/(p+1)}(1-x)^{4/(p-1)-k}\phi(x)G(x)\,dx}{\int_0^1 x^{(2p+4)/(p+1)}(1-x)^{4/(p-1)}\phi(x)\,dx} \tag{44}$$

where

$$G(\xi) = \frac{p+1}{2}\xi^{(p+3)/(p+1)}(1-\xi)^k \times \int_0^1 \frac{(1-x^{(p+1)/2})z(\xi x^{(p+1)/2})}{(1-\xi x^{(p+1)/2})^{k+2}}\,dx, \tag{45}$$

$$0 \le \xi < 1, \quad G(1) = f(1)$$

Now the scheme for successive iterations can be presented as follows,

1. Select initial $f_0'(0)$ and $z_0(\xi)$.
2. Update $f_i(\xi)$ according to (42) by using $f_i'(0)$ and $z_i(\xi)$.
3. Update $\phi_i(\xi)$ according to (40) by using $f_{i+1}(\xi)$ and $z_i(\xi)$.
4. Update $z_i(\xi)$ according to (43) by using $f_{i+1}(\xi)$ and $\phi_{i+1}(\xi)$.
5. Update $f_i'(0)$ according to (44) and (45) by using $z_{i+1}(\xi)$ and $\phi_{i+1}(\xi)$.
6. If a given accuracy is not satisfied, go back to Step 2.

Once $f$ and $z$ have been obtained for a given accuracy, one can find parameter $\beta$ from (41). Then the optimum eigenvalue $\lambda$, function $\phi_u$, and the optimum $\alpha$ can be obtained according to (18), (40), and (17), respectively. The linear dimension of the beam of the optimum manipulator is $\alpha^{1/p}(\xi)$.

### 5.3. *Case* $p > 1$ *and* $\eta \neq 0$

In this case, we only need to take care of the singularity of $u$ at $\xi = 1$. To this end, we introduce two new functions by,

$$f(\xi) = (1-\xi)^k u(\xi), \quad z(\xi) = (1-\xi)^{k+2}u''(\xi). \tag{46}$$

Again, $k$ is the singularity of $u$ at $\xi = 1$ determined from (24). Both $f$ and $z$ are regular over the entire interval $0 \le \xi \le 1$, and

$$f(0) = 0, \quad f'(0) = u'(0), \qquad f(1) = \frac{z(1)}{k(k+1)}. \tag{47}$$

In terms of $f$ and $z$, function $\phi_u$ and parameter $\beta$ can be rewritten as,

$$\phi_u(\xi) = (1-\xi)^{4/(p-1)}\phi(\xi),$$
$$\phi(\xi) = \left[\frac{f^2(\xi) + (1-\xi)^{2k}}{z^2(\xi)}\right]^{1/(p-1)}, \tag{48}$$
$$\beta = \int_0^1 (1-\xi)^{4/(p-1)}\phi(\xi)\,d\xi.$$

From eqs. (46), (28), and (30) we get,

$$f(\xi) = \xi(1-\xi)^k\left[f'(0) + \xi\int_0^1 \frac{(1-x)z(x\xi)}{(1-x\xi)^{k+2}}\,dx\right], \quad 0 \le \xi < 1. \tag{49}$$

$$z(\xi) = \frac{s\left[f^2(\xi) + (1-\xi)^{2k}\right]^{\frac{p}{p+1}}}{\left|\begin{array}{l} p\int_0^1 x(1-x)^{4/(p-1)-k}\phi[\xi + x(1-\xi)] \\ \quad \times f[\xi + x(1-\xi)]\,dx \end{array}\right|^{(p-1)(p+1)}} \tag{50}$$

where $s$ is the sign of the denominator. From the second equation of boundary conditions (16) we find,

$$f'(0) = -\frac{z(0)}{p\eta\beta|z(0)|^{\frac{2p}{p-1}}}. \tag{51}$$

Now the scheme for successive iterations can be specified as follows:

1. Select an initial $\beta_0$ and an initial $z_0(\xi)$.
2. Update $f_i(\xi)$ according to (49) and (51) by using $\beta_i$ and $z_i(\xi)$.
3. Update $\phi_i(\xi)$ according to (48) by using $f_{i+1}(\xi)$ and $z_i(\xi)$.
4. Update $z_i(\xi)$ according to (50) by using $f_{i+1}(\xi)$ and $\phi_{i+1}(\xi)$.
5. Update $\beta_i$ according to (48) by using $f_{i+1}(\xi)$ and $z_{i+1}(\xi)$.
6. If a given accuracy is not satisfied, go back to Step 2.

Once $\beta$, $f$, and $z$ have been determined within the specified accuracy, one can find the optimum eigenvalue $\lambda$, function $\phi_u$, and then the optimum $\alpha$, according to (18), (48), and (17), respectively.

**Table 1. Ratio of $\sqrt{\lambda}/\lambda_c$ for Various Values of $\eta$ ($p = 2, 3$)**

| | $\eta = 0$ | $\eta$ =0.1 | $\eta$ =0.5 | $\eta$ =1.0 | $\eta$ =10 | $\eta = \infty$ |
|---|---|---|---|---|---|---|
| $p = 2$ | 2.9492 | 3.8626 | 5.6396 | 6.1888 | 6.9039 | 7.0025 |
| | Fig. 1*A* | Fig. 1*B* | Fig. 1*C* | Fig. 1*D* | Fig. 1*E* | Fig. 1*F* |
| $p = 3$ | 2.1298 | 2.4873 | 3.5799 | 3.8638 | 4.2393 | 4.2937 |
| | Fig. 2*A* | Fig. 2*B* | Fig. 2*C* | Fig. 2*D* | Fig. 2*E* | Fig. 2*F* |

## 6. Numeric Examples and Discussions

Numeric analysis has been conducted using the successive iteration schemes described in the previous section. We present some of the results here for $p = 2$ and $p = 3$.

The successive iteration processes are controlled by the following accuracy criteria,

$$\frac{|f'_{i+1} - f'_i|}{|f'_{i+1}|} + \frac{\|f_{i+1} - f_i\|}{\|f_{i+1}\|} + \frac{\|z_{i+1} - z_i\|}{\|z_{i+1}\|} < \epsilon,$$

and

$$\frac{|\beta_{i+1} - \beta_i|}{|\beta_{i+1}|} + \frac{\|f_{i+1} - f_i\|}{\|f_{i+1}\|} + \frac{\|z_{i+1} - z_i\|}{\|z_{i+1}\|} < \epsilon$$

for $\eta = 0$ and $\eta \neq 0$, respectively.

To simplify the numeric computation, we have approximated all functions by splines by interpolating at $N + 1$ uniformly distributed discrete points on $0 \leq \xi \leq 1$. Throughout the entire section, $N = 10$ and $\epsilon = 10^{-4}$ are used in all computations. All numeric integrations are carried out by using the recursive Simpson's formula.

For $\eta = 0$, the iteration for $f'(0)$ and $z(\xi)$ starts with $f'_0(0) = -1$ and $z_0(\xi) = 1$, and convergence is achieved after 25 iterations for $p = 2$ and 26 for $p = 3$. For $\eta \neq 0$, the iteration for $\beta$ and $z(\xi)$ starts with $\beta_0 = 1$ and $z_0(\xi) = 1$. In this case, for large $\eta$ (say, $\eta = 100$), convergence is achieved after 34 iterations for $p = 2$ and 16 for $p = 3$. For small $\eta$ (say, $0.5 \leq \eta \leq 1$), the iteration process converges very slowly (about 1000 iterations), and for $\eta \leq 0.5$, it does not converge at all with the initial guesses $\beta_0 = 1$ and $z_0(\xi) = 1$. This problem can be solved by using the converged $\beta$ and $z(\xi)$ of the previous value of $\eta$ as the initial guesses of $\beta_0$ and $z_0(\xi)$ for the new $\eta$ value, however, the speed of convergence is still very slow and becomes extremely slow for $\eta \leq 0.1$.

For various $\eta$ values, Table 1 summarizes the increase in the fundamental frequency in comparison with that of a flexible manipulator with a beam of uniform cross section and the same length, volume, and material as the optimum flexible manipulator.

Figure 1 illustrates the optimal linear dimension (e.g., radius of the cross sections) of the geometrically similar cross sections ($p = 2$). Figure 2 gives the same results for the rectangular cross sections of given uniform width

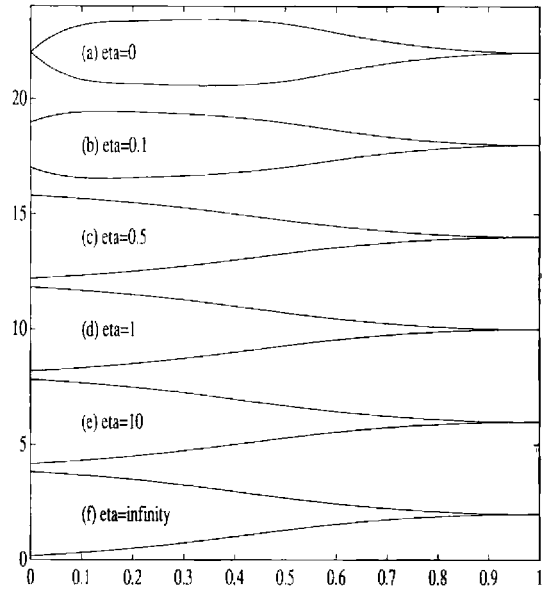


*Fig. 1. Optimum tapering of geometrically similar cross section ($p = 2$).*

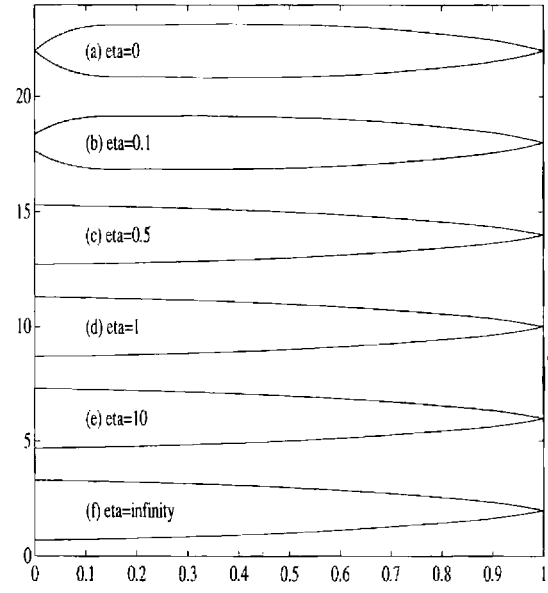


*Fig. 2. Optimum tapering of rectangular cross section of given width ($p = 3$).*

($p = 3$). Both figures indicate that the optimal cross sections shrink to zero at the clamped end as $\eta$ approaches zero but obtain their maximum value there for $\eta \geq 0.5$. Physically, it is very clear that the mass concentration near the clamped end would increase the vibration frequency of a flexible manipulator.

Figure 3 presents the relationship between the fundamental frequency $\sqrt{\lambda}$ and hub inertia $\eta$ for an optimal flexible manipulator. The dashed curve in the figure is the

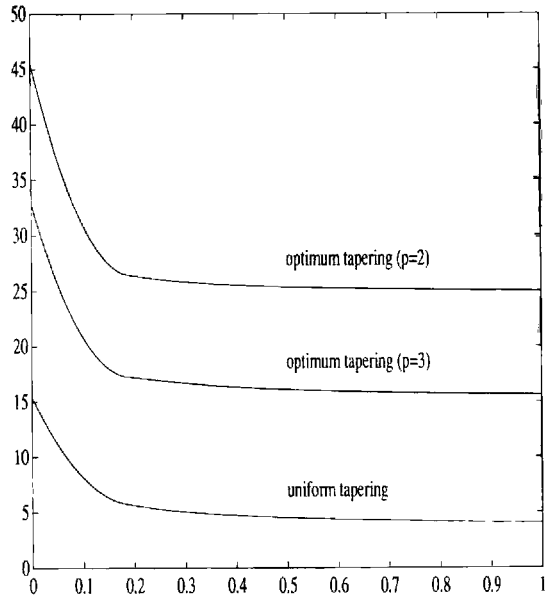


*Fig. 3. Fundamental frequencies vs. hub inertia parameter $\eta$ ($p = 2, 3$).*

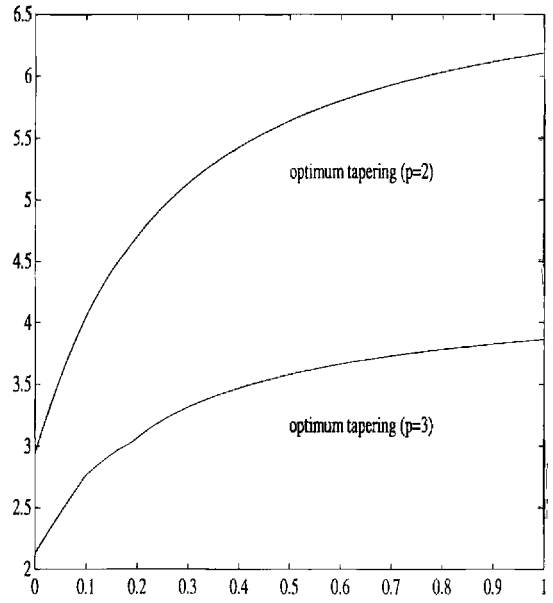


*Fig. 4. Ratio of $\sqrt{\lambda}/\lambda_c$ vs. hub inertia parameter $\eta$ ($p = 2, 3$).*

result obtained from eq. (3) for the corresponding manipulator with a beam of uniform cross section. From those curves, one can find that the optimal fundamental frequency of a flexible manipulator is sensitive with respect to the change in the hub inertia for small $\eta$ ($\eta \leq 0.2$).

The increase in the fundamental frequency achieved through the optimum design is depicted in Figure 4. Clearly, the increment decreases as hub inertia $\eta$ decreases.

## 7. Sensitivity Analysis of Optimal Fundamental Frequencies

To obtain some useful information on the machining allowance for making an optimum manipulator, we must know the effect of small changes in the hub inertia on the value of the optimal fundamental frequency. To this end, we introduce an index to measure the sensitivity of the optimal frequency with respect to the variation of hub inertia $\eta$.

From eq. (6), the change of $\omega^2$ due to variations in $EJ$, $\rho A$, and $I_H$ can be found as

$$\delta\omega^2 = \frac{\int_0^L \delta(EI)v''^2 dx}{\int_0^L \rho A v^2 dx + I_H v'(0)^2} - \omega^2 \frac{\int_0^L \delta(\rho A)v^2 dx + \delta I_H v'(0)^2}{\int_0^L \rho A v^2 dx + I_H v'(0)^2}. \tag{52}$$

Note that although $\delta(EJ)$, $\delta(\rho A)$, and $\delta I_H$ cause a corresponding variation $\delta v$ in $v$, $\delta v$ will not affect the value of $\omega$, since $\omega$ obtains its minimum value at $v$. This is why we do not need to consider $\delta v$ in expression (52). For the optimal frequency, since both $\alpha$ and $u$ make $\lambda$ achieve its extremal value, their variations around the optimal solution will not change the value of $\lambda$. Hence eq. (52) becomes

$$\delta\lambda = -\lambda \frac{u'(0)^2}{\int_0^1 \alpha u^2 d\xi + \eta u'(0)^2} \delta\eta. \tag{53}$$

Define a *sensitivity index* of $\lambda$ with respect to $\eta$ by,

$$S_\eta \equiv \frac{\%\text{ change in } \lambda}{\%\text{ change in } \eta} = \frac{\delta\lambda/\lambda}{\delta\eta/\eta} = \frac{\eta}{\lambda}\frac{\delta\lambda}{\delta\eta} S_\eta = -\frac{\eta u'(0)^2}{\int_0^1 \alpha u^2 d\xi + \eta u'(0)^2}. \tag{54}$$

Clearly, $-1 \leq S_\eta \leq 0$, and thus the optimal frequency is not very sensitive to the hub inertia variation. Table 2 lists the value of the sensitivity index for various $\eta$. Note that $S_\eta = 0$ for $\eta = \infty$, not $-1$, as one may have expected from eq. (54). This can be verified from identity (19). As $\eta$ approaches $\infty$, this identity will take the same form as that of eq. (21). Hence from (19), $\eta u'(0)^2$ approaches zero as $\eta$ goes to $\infty$, and accordingly, $S_\eta = 0$ for $\eta = \infty$.

Figure 5 presents the $S_\eta$-*versus*-$\eta$ curve. Clearly, the optimal fundamental frequency is more sensitive to the variation of hub inertia when $\eta$ is small. As illustrated in Figure 5*A*, $S_\eta$ varies dramatically in the range of $0 \leq \eta \leq 0.25$.

**Table 2. Sensitivity Index $S_\eta$ for Various Values of $\eta$ ($p = 2,\ 3$)**

| | $\eta = 0$ | $\eta$ =0.1 | $\eta = 0.5$ | $\eta$ =1.0 | $\eta = 100$ | $\eta = \infty$ |
|---|---|---|---|---|---|---|
| $p = 2$ | 0.0 | -0.9881 | -0.9335 | -0.8619 | -0.0525 | 0.0 |
| $p = 3$ | 0.0 | -0.9829 | -0.9210 | -0.8351 | -0.0413 | 0.0 |

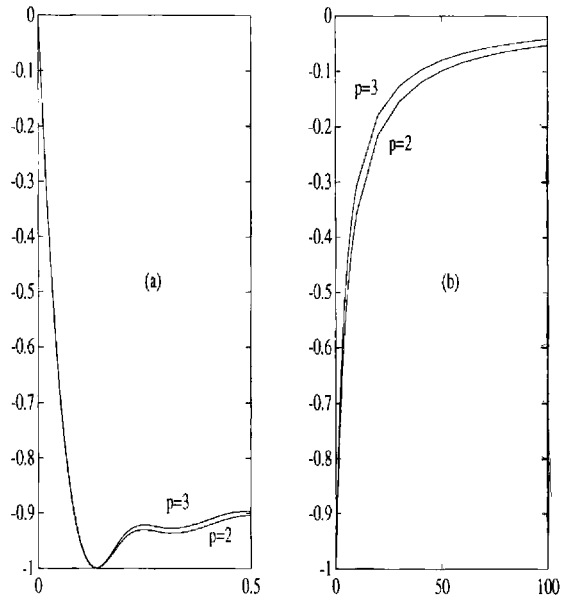


*Fig. 5. Sensitivity index $S_\eta$ vs. hub inertia parameter $\eta$ ($p = 2, 3$).*

## 8. Conclusion

The problem of optimum shape design of a flexible manipulator has been formulated and solved by the successive iteration schemes. A substantial increase in the fundamental frequency has been found in the numeric analyses. This will enable the flexible manipulator to move faster without causing serious vibration problems at its end point, thus improving the position precision and productivity. Sensitivity analysis has indicated that the optimal frequency is not very sensitive to the variation in hub inertia.

As the numeric results have indicated, the optimal beam tapering can lead to zero-area cross sections. This situation may not be allowed in most applications and can be remedied by imposing a positive lower bound on the shape function. Additional requirements, such as an upper bound, can also be introduced into the problem formulation. These constraints, however, will make analytical analysis extremely difficult, if not impossible, and some numeric optimization method must be used to find the optimum design. Some initial results along this direction have been recently obtained (Wang and Russell 1992). New results on the dual optimum design problem of finding the minimum-weight robot arm for a specified fundamental frequency are given in Wang and Russell (1993).

## Acknowledgment

This work was supported in part by a grant from the University of Arizona Foundation and the Office of the Vice President for Research.

## References

Asada, H., Park, J.-H., and Rai, S. 1991. A control-configured flexible arm: Integrated structure/control design. In *Proc. of IEEE Conf. on Robotics and Automation*. Sacramento: IEEE, pp. 2356–2362.

Bellezze, F., Lanari, L., and Ulivi, G. 1990. Exact modeling of the flexible slewing link. In *Proc. of IEEE Conf. on Robotics and Automation*. Cincinnati: IEEE, pp. 734–739.

Karihaloo, B. L., and Niordson, F. I. 1973. Optimum design of vibrating cantilevers. *J. Optimization Theory Applications* 11(6):638–654.

Niordson, F. I. 1965. On the optimal design of a vibrating beam. *Q. Appl. Mathematics* 23(1):47–53.

Schwarz, B. 1962. Some results on the frequencies of nonhomogeneous rods. *J. Math. Analysis Applications* 5(1):169.

Wang, F.-Y. 1991. Optimum design of vibrating cantilevers: A classical problem revisited. *J. Optimization Theory Applications*, in press.

Wang, F.-Y., and Kwan, O. 1993. Influence of rotatory inertia, shear deformation and loading on vibration behaviors of flexible manipulators. *J. Sound Vibrations* 167(2):1–15.

Wang, F.-Y., and Russell, J. L. 1992. Minimax optimum shape construction of flexible manipulators with tip loads. In *Proc. of IEEE Int. Conf. on Decision and Control*. Tucson: IEEE, pp. 311–316.

Wang, F.-Y., and Russell, J. L. 1993. Minimum-weight robot arm for a specified fundamental frequency. In *Proc. of IEEE Conf. on Robotics and Automation*. Atlanta: IEEE, pp. 490–495.